Skin friction distribution along driven piles

La distribution de la résistance latérale le long des pieux enfoncés

R.C.JOSHI, Professor, Department of Civil Engineering, University of Calgary, Calgary, Canada
H.D.SHARMA, Adjunct Professor, Department of Civil Engineering, University of Calgary, Calgary, Canada, and Technical Specialist, (Principal Engineer) Fluor, Calgary, Canada Ltd, Canada
D.SPARROW, Graduate Student, Department of Civil Engineering, University of Calgary, Calgary , Canada

SYNOPSIS: This paper presents the details of a model pile testing equipment and the results of load tests conducted on instrumented model piles in sand. The equipment consisted of two cylindrical tanks, one for sand deposition and the other for testing of model piles. Results of load tests on instrumented driven model piles, interpretation of the test data, comparison of failure loads with empirically determined loads and the conclusions regarding skin friction mobilization are also included.

INTRODUCTION

The bearing capacity of piles in sand has been studied for many decades (Hann and Tan, 1973, Kerisel, 1961, and Vesic, 1964 and 1970). There still exists a great deal of uncertainty regarding the selection of appropriate values for end bearing and also distribution of skin friction along the pile shaft.

The present series of model tests employ precision strain gauges along the length of the pile and high caliber load cells at the top and bottom of the pile.

The analysis of bearing capacity was based on the static approach where the ultimate load, Q_o, is the sum of the point load, Q_p, and the skin load, Q_s:

$$Q_o = Q_p + Q_s = q_o A_p + f_o A_s \qquad (1)$$

where A_p and A_s represent the point bearing area and the skin bearing area, respectively; and q_o and f_o represent the unit point resistance and unit skin resistance respectively. These unit resistances are based on rigid-plastic solid theory and expressed as:

$$q_o = \bar{p} N_q \qquad (2)$$

$$f_o = \tfrac{1}{2} \bar{p} k_s \tan\delta \qquad (3)$$

where $\bar{p}$ is the effective overburden pressure; N_q is the bearing capacity factor; k_s is the coefficient of earth pressure and δ^s is the soil pile friction angle. From the pile load tests the values of q_o and f_o were obtained. Modified direct shear tests were performed to determine the value of the soil-pile friction angle. Tests were performed on model piles with length, L, to diameter, D, ratios of 16 to 33. This paper presents the details of test apparatus, testing equipment, test data and their interpretation.

APPARATUS AND TESTING

Sand Properties

The sand used was an air dried masonary sand. It had a uniformity coefficient of 2.42, an effective size of 0.9 mm and a Unified Soil Classification of SP-SM. The soil friction angle at a density of 17.0 kN/m³ obtained from direct shear tests was found to be 43°. It had a maximum dry density of 17.93 kN/m³ and a minimum dry density of 15.98 kN/m³.

Sample Preparation:

The sand bed was prepared by a technique known as pluviation or raining. The basic principle of operation is similar to one described by Rad and Tumay (1987). Figure 1 shows a schematic diagram of the apparatus used to prepare the sand bed for pile installation.

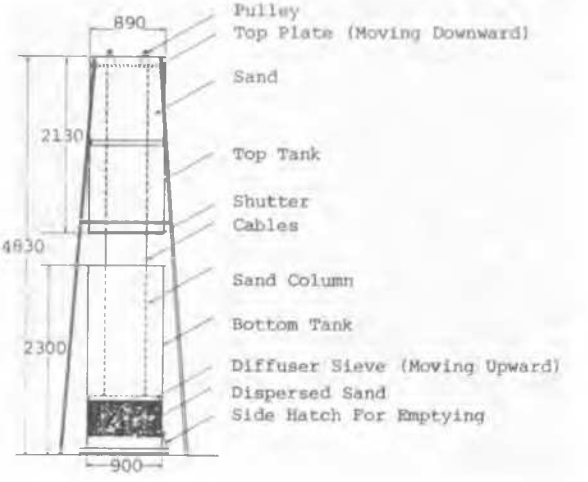

Figure 1. Schematic drawing of sand raining apparatus.

To begin preparation the top tank measuring 2.13 m in height and 0.89 m in diameter was filled with sand. A steel plate, which was 0.87 m in diameter, was then placed over the sand. The bottom tank measuring 2.10 m in height and 0.914 m in diameter was then placed under the top tank. The diffuser sieve was placed inside the bottom tank and connected to cables; these cables ran over pulleys fixed to the upper rim of the top tank, and were then attached to the top plate. The diffuser consisted of two sieves rotated 45° with respect to each other spaced 50 mm apart with a nominal sieve opening size of 6.35 mm. The diameter of the diffuser was 0.90 m. A dust shroud was employed between the two tanks to eliminate the generation of dust.

To begin the filling the shutter on the bottom of the top tank was opened. The shutter consisted of a 9.5 mm thick steel plate with uniformly spaced 12.7 mm holes and a total porosity of 3.61%. The base of the top tank had a similar hole pattern. The shutter was connected to the base of the tank by a nut and bolt arrangement via a channel in the shutter, this enabled movement of the shutter in one horizontal direction. When open the two sets of holes lined up and the sand rained from the top tank. When the shutter was closed the holes were offset and the sand was retained in the top tank. As sand passed through the holes in the shutter, the volume of sand in the top tank decreased, and the top plate moved downward. The downward movement of the top plate raised the diffuser and kept the falling height, the distance that the sand traveled from the bottom of the diffuser before being deposited, constant at 0.394 m. This resulted in samples of a homogeneous cross-section and uniform density of 17.17 kN/m^3 or 69% relative density as well as a soil fabric similar to the one found in natural deposits formed by sedimentation.

Pile Design:

The pile was constructed of a 1026 cold rolled mild steel seamless pipe of 50.8 mm outside diameter and 2.54 mm wall thickness. The pile was assembled in sections using threaded connections with 24 threads per inch. This allowed strain gauges to be placed along the inside wall of the pile as well as enabling the length to be altered for testing various L/D ratios. The bottom section of the pile also contained a 10 kN load cell fabricated at The University of Calgary for measuring the point load. Each pile section had an inside slot 38 mm wide where the wall thickness was reamed to 0.64 mm; here the strain gauges were mounted to ensure precise strain measurements at low loads. Each pile section had two precision electrical resistant strain gauges mounted diagonally opposite to each other. A pile cap was attached to the top pile section for driving and pile loading.

Pile Driving:

Once the sand bed was prepared the top tank was removed and the pile driving apparatus set up on top of the test tank. The pile was then placed in the guides positioned along the hammer channel. These guides could be repositioned as the pile was driven to ensure the pile was always being driven straight.

The driving was achieved by the traditional rope and pulley arrangement. The hammer weighed 10.7 kg and was dropped 0.30 m each blow. This imparted a constant energy of 32.0 J.

Pile Loading and Data Acquisition:

Pile loading was achieved using a MTS closed loop testing system. This employed a 40 kN double acting hydraulic actuator. Attached to the bottom of the ram was a 50 kN load cell to measure applied load. Displacement measurements were made by a linear variable differential transformer (LVDT) in the actuator. Data acquisition was accomplished using a Fluke Helios 1 and a Zenith 150 personal computer.

Pile Loading Methods:

The initial part of the test program involved performing load tests by three different loading methods on the same L/D ratio. Three test methods, namely, the Slow Maintained Load (Slow ML) test method, the Constant Rate of Penetration (CRP) test method, and the Quick Maintained Load (Quick ML) test method were adopted to test the model piles. However, due to lack of space only data from CRP tests on piles of different L/D ratios are presented.

In the CRP test method the pile was forced to settle at 0.5 mm/min and the force required to achieve the penetration was recorded.

TEST RESULTS AND DISCUSSION

Ultimate Loads and Displacements:

The displacement of the pile head versus top load for the various L/D ratios studied are shown in Figure 2. The curves are similar in shape to those seen in previous full scale (Travenas, 1971 and Vesic, 1970) and model tests (Hanna and Tan, 1973, Kerisel, 1961 and Vesic, 1963 and 1964) and consist of initial linear sections which gradually turn to final linear sections with steadily increasing load. The ultimate load has been defined as the load corresponding to 10% of the pile diameter displacement.

The displacement of the pile head versus point load can be seen in Figure 3. The maximum value of the point load was defined as described above for the total load curve. It should be noted that the total and point load versus displacement curves are almost identical in shape. Full point load was mobilized between 5-6 mm displacement for all L/D ratios confirming Vesic's (1964) results that full point mobilization occurs at a displacement that is a function of foundation width and placement method.

The curves for the skin load versus displacement, Figure 4, are similar in shape to the previous two sets of curves except for the L/D=28 curve. The final linear section for L/D=28 was a bit steeper than the other curves. This is possible due to experimental

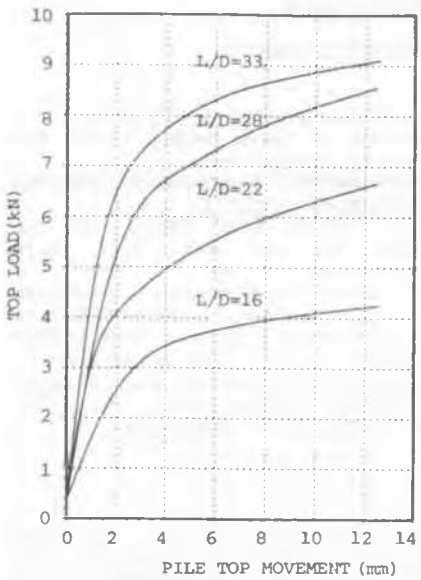

Figure 2. Top load versus pile top movement for L/D ratios tested.

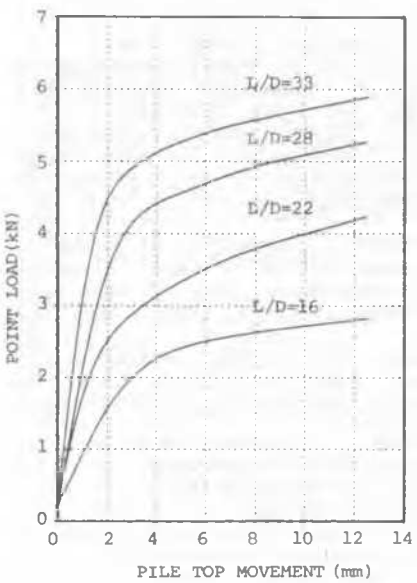

Figure 3. Point load versus pile top movement for L/D ratios tested.

error. Except for the L/D=28 curve the remaining developed their full skin resistance after a settlement of 8-9 mm, again confirming Vesic's (1964) earlier findings that the displacement necessary for full skin mobilization is independent of pile dimensions.

Point and Skin Resistance Analysis

The ultimate point load does not reach a constant value up to L/D = 33. Model tests

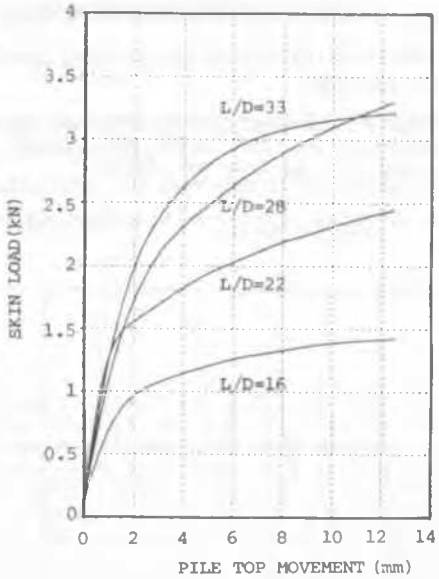

Figure 4. Skin load versus pile top movement for L/D ratios tested.

performed by Vesic (1964) on 102 mm diameter piles in dry dense sand ultimate point and skin resistances reached constant values at L/D ratios of approximately 30. Furthermore, the L/D ratio at which constant values occurred were a function of relative density. Full scale pile tests (Tavenas 1971, Vesic, 1970,) have found the ultimate point and skin resistances to reach constant values at L/D ratios of 20-30.

The ultimate skin resistance reaches a constant value at an L/D ratio of approximately 21. This compares favourable with the findings of others. End effects could have been a possible reason why the unit point resistance failed to reach a constant value. The distance between the bottom of the tank and the end of the pile for the L/D = 33 was equal to 6 pile diameters. According to Meyerhof (1959) the influence of pile driving in dense sand, on the relative density of the sand is insignificant beyond 5 pile diameters below the base of the pile.

Randolph (1985) attributes the limiting values of end bearing and skin friction to the gradual reduction of friction angle with increased confining pressure and not to a form of arching as previously thought. The maximum embedment depth in this test series was only 1.68 m, far too small to create confining pressures capable of suppressing the dilation of the sand and corresponding high friction angles. Although contrary to the finds of Kerisel's (1961) and Vesic's (1964) model tests it may offer a rational explanation as to why a constant point resistance was not achieved. It should also be pointed out that Vesic's embedment depths exceeded 3 meters and Kerisel's were 7 meters. This however does not explain why a constant skin resistance was reached and not a constant point resistance. Perhaps the variation of earth pressure coefficient with depth was greater than the variation of sand friction angle, resulting in

the limiting depth for the skin resistance.

Distribution of Pile Load

Figure 5 shows the axial load distribution in the pile for selected applied loads for pile with L/D=33 for the CRP loading procedure.

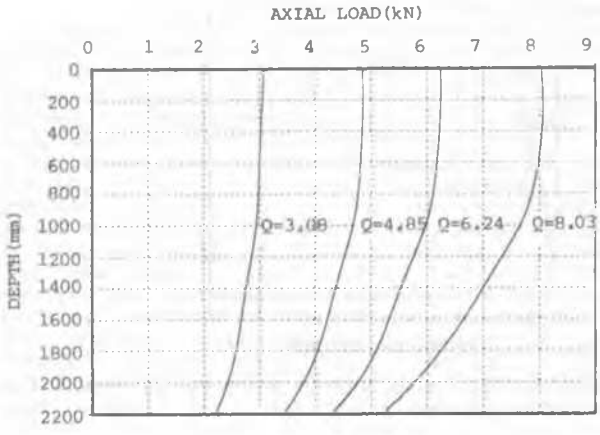

Figure 5. Axial load distribution for L/D=33.

Similar trend was recorded for other piles with other L/D ratios. The loads were computed from

$$P = AE\varepsilon \qquad (4)$$

where P = average load at the center of the strain gauge span; A = cross section area of the pile where the gauges were located; ε = the strain which was the average of the two diagonally opposite gauges; and E = the modulus of elasticity of the pile material. The shape of the curves are identical for the three test methods. They also compare favourable with the shape of the curves obtained from other full scale and model pile tests (Hanna and Tan, 1973, Tavenas, 1971, Vesic, 1970). Since pile deformation was insignificant almost all the displacement of the pile head was seen at the pile toe enabling mobilization of substantial point load early in the test because of the relative displacement between the point and the adjacent soil. This is often not the case with full size deformable piles and explains why the skin friction distribution curve is generally parabolic. The skin friction in the upper part of the pile is mobilized much earlier than that in the lower portion of the pile. As a result of the low pile deformation and corresponding high relative displacement between pile point and adjacent soil the skin friction distribution was found to be basically triangular. The skin friction distribution was obtained by differentiating the axial load distribution curve:

$$f_o = \frac{-1}{P} \frac{dQ}{dz} \qquad (5)$$

where f_o = skin resistance; P = pile perimeter length = $2\pi r$; r = pile radius; and $\frac{dQ}{dz}$ = change of axial load with depth.

CONCLUSIONS

Based on the results of these model tests the following conclusions can be made:

1. All three loading procedures produce similar load displacement curves.
2. Full point load was found to be mobilized between 5-6 mm and full skin friction between 8-9 mm.
3. Ultimate skin resistance remained constant beyond a L/D ratio of approximately 21 while the ultimate point resistance continued to increase up to a L/D ratio of 33.
4. The axial load distribution was similar for all L/D ratios. The skin friction distribution was found to be triangular.

ACKNOWLEDGEMENTS

The authors are grateful to the National Research Council of Canada for funding this research project. Also special thanks to the laboratory technicians for their invaluable input and assistance.

REFERENCES

Hanna, T.H. and Tan, R.H.S. (1973). The Behavior of Long Piles Under Compressive Loads in Sand. Canadian Geotechnical Journal, Vol. 10, No. 3, pp. 311-340.

Kerisel, J. (1961). Fondations Profondes En Milieu Sableux. Proceedings of the Fifth International Conference on Soil Mechanics and Foundation Engineering, Paris, Vol. II, pp. 73-83.

Meyerhof, G.G. (1959). Compaction of Sands and Bearing Capacity of Piles. Journal of the Soil Mechanics and Foundations Engineering Division, ASCE, Vol. 85, No. SM6, pp. 1-29.

Rad, N.S. and Tumay, M.T. (1987). Factors Affecting Sand Specimen Preparation by Raining. Geotechnical Testing Journal, Vol. 10, No. 1, pp. 31-37.

Randolph, M.F. (1985). Capacity of Piles Driven Into Dense Sand. Cambridge University, Dept. of Engineering, CUED/D-SOILS/TR-171, 32 pp.

Tavenas, F. (1971). Load Tests on Friction Piles In Sand. Canadian Geotechnical Journal, Vol. 8. No. 1, pp. 7-22.

Vesic, A.S. (1963). Bearing Capacity of Deep Foundation In Sand. National Academy of Sciences, National Research Council, Highway Research Record 39, pp. 112-153.

Vesic, A.S. (1964). Investigations of Bearing Capacity of Piles In Sand. North American Conference on Deep Foundations, Mexico City.

Vesic, A.S. (1970). Tests on Instrumented Piles, Ogeechee River Site. Journal of the Soil Mechanics and Foundations Division, ASCE, Vol. 96, No. SM2, pp. 561-583.